

Structural relaxation in amorphous materials under cyclic tension-compression loading

Pritam Kumar Jana^{1,2} and Nikolai V. Priezjev³

¹*Institut für Theoretische Physik, Universität Göttingen,
Friedrich-Hund-Platz 1, 37077 Göttingen, Germany*

²*Universite Libre de Bruxelles (ULB),
Interdisciplinary Center for Nonlinear Phenomena and Complex Systems,
Campus Plaine, CP 231, Blvd. du Triomphe, B-1050 Brussels, Belgium and*

³*Department of Mechanical and Materials Engineering,
Wright State University, Dayton, OH 45435*

(Dated: December 3, 2019)

Abstract

The process of structural relaxation in disordered solids subjected to repeated tension-compression loading is studied using molecular dynamics simulations. The binary glass is prepared by rapid cooling well below the glass transition temperature and then periodically strained at constant volume. We find that the amorphous system is relocated to progressively lower potential energy states during hundreds of cycles, and the energy levels become deeper upon approaching critical strain amplitude from below. The decrease in potential energy is associated with collective nonaffine rearrangements of atoms, and their rescaled probability distribution becomes independent of the cycle number at sufficiently large time intervals. It is also shown that yielding during startup shear deformation occurs at larger values of the stress overshoot in samples that were cyclically loaded at higher strain amplitudes. These results might be useful for mechanical processing of amorphous alloys in order to reduce their energy and increase chemical resistivity and resistance to crystallization.

Keywords: metallic glasses, periodic deformation, yield stress, molecular dynamics simulations

I. INTRODUCTION

The advancement of processing methods and characterization techniques is crucial for the rational design of amorphous alloys with a combination of desired properties, involving strength, plasticity, corrosion resistance, and wear resistance [1]. It is well realized that the exceptionally high strength, thermoplastic formability, and excellent magnetic properties make metallic glasses suitable for numerous structural, biomedical, and magnetic applications [1]. In contrast to crystalline materials, metallic glasses are characterized by an amorphous structure, and their elementary plastic deformation involves swift rearrangements of small groups of atoms, or shear transformations [2, 3]. A major obstacle for the widespread use of metallic glasses, however, is the strain localization within narrow bands, and, as a result, a failure of the material under applied strain [4]. Depending on a technological application, various thermo-mechanical processing methods might be required to either relax the system to lower energy states or rejuvenate the glass to higher energies [5]. Examples of the most common methods include high-pressure torsion, wire drawing, shot peening, cryogenic thermal cycling, elastostatic loading, and cyclic loading [5]. However, despite significant progress, it remains unclear if extreme relaxation or rejuvenation can be achieved using a combination of these methods; for example, alternating mechanical agitation and thermal cycling.

During the last decade, a number of atomistic simulation studies were carried out to investigate the relaxation dynamics, the range of accessible energy states, and mechanical properties of periodically deformed amorphous materials [6–28]. In general, it was found that the yielding transition occurs after a number of transient cycles, depending on the preparation history, strain amplitude and temperature, and, in addition, it is accompanied by the formation of the system-spanning shear band and a sudden decrease in the stress amplitude [15, 16, 21, 28]. On the other hand, cyclic loading at strain amplitudes below the critical value can be termed as ‘mechanical annealing’, which leads to progressively lower potential energy states over consecutive cycles [7, 19, 21, 22, 27]. In the limiting case of athermal quasistatic periodic loading, amorphous systems eventually reach the state with the lowest energy, the so-called limit cycle, where the particle dynamics becomes exactly reversible [7, 8]. Interestingly, it was recently shown that structural relaxation in amorphous solids is accelerated when an additional shear orientation is introduced in the periodic defor-

mation protocol, which leads to the increase in strength and shear-modulus anisotropy [27]. Nevertheless, a detailed description of the structural relaxation process during cyclic loading is still missing.

In this paper, the influence of time-periodic tension-compression loading on structural relaxation in amorphous alloys is investigated using molecular dynamics simulations. The binary alloy is first rapidly cooled from the liquid state to a temperature well below the glass transition point, and then periodically strained at constant volume during hundreds of cycles. It will be shown that cyclic loading in the elastic range results in lower energy states when samples are strained at higher strain amplitudes. The relaxation proceeds via large-scale collective nonaffine displacements of atoms, and their rescaled probability distribution becomes independent of the cycle number. The mechanical tests during startup deformation indicate that the stress overshoot and shear modulus are increased for samples cyclically loaded at larger strain amplitudes.

The remainder of the paper is structured as follows. The details of the simulation model and deformation protocol are described in the next section. The time evolution of the potential energy, as well as the analysis of nonaffine displacements, and the effect of cyclic loading on mechanical properties are presented in section III. The results are briefly summarized in the last section.

II. MOLECULAR DYNAMICS SIMULATIONS

The three-dimensional amorphous material is modeled via the Kob-Andersen (KA) binary (80:20) Lennard-Jones (LJ) mixture [29]. In the KA model, the interaction between atoms of different types is strongly non-additive, which impedes crystallization at low temperatures [29]. The phase diagram of the KA mixture is well known, and the model is frequently employed to study the structural and dynamical properties of glass formers [29]. More specifically, the LJ interaction between atoms of types $\alpha, \beta = A, B$ is defined as follows:

$$V_{\alpha\beta}(r) = 4\varepsilon_{\alpha\beta} \left[\left(\frac{\sigma_{\alpha\beta}}{r} \right)^{12} - \left(\frac{\sigma_{\alpha\beta}}{r} \right)^6 \right], \quad (1)$$

where $\varepsilon_{AA} = 1.0$, $\varepsilon_{AB} = 1.5$, $\varepsilon_{BB} = 0.5$, $\sigma_{AA} = 1.0$, $\sigma_{AB} = 0.8$, $\sigma_{BB} = 0.88$, and $m_A = m_B$ [29]. All MD simulations were performed using the LAMMPS parallel code and a relatively large system of 60 000 atoms [30]. In order to reduce the computational time, we

use the cutoff radius $r_{c,\alpha\beta} = 2.5\sigma_{\alpha\beta}$. Unless noted otherwise, the physical quantities are expressed in the reduced LJ units of length, mass, and energy $\sigma = \sigma_{AA}$, $m = m_A$, $\varepsilon = \varepsilon_{AA}$, and, consequently, time $\tau = \sigma\sqrt{m/\varepsilon}$. The integration time step in the velocity-Verlet scheme is $\Delta t_{MD} = 0.005\tau$.

The preparation of the poorly annealed glass was performed as follows. First, the LJ mixture was equilibrated at the high temperature $T_{LJ} = 1.0\varepsilon/k_B$ and density $\rho = \rho_A + \rho_B = 1.2\sigma^{-3}$. In the following, the parameters k_B and T_{LJ} denote the Boltzmann constant and temperature, respectively. The system temperature was regulated through the Nosé-Hoover thermostat [30, 31]. The critical temperature of the KA model is $T_c = 0.435\varepsilon/k_B$ at $\rho = 1.2\sigma^{-3}$, which was determined by fitting the diffusion coefficient to a power-law function upon approaching the glass transition [29]. The linear size of the undeformed cubic box is $L = 36.84\sigma$ at the density $\rho = 1.2\sigma^{-3}$. Following the equilibration period, the binary mixture was rapidly cooled to the temperature $T_{LJ} = 0.01\varepsilon/k_B$ with the rate $10^{-2}\varepsilon/k_B\tau$, while keeping the volume constant. This preparation procedure is identical to the one considered in the recent study on cyclic loading with alternating shear orientation [27].

After the preparation phase, the glass was periodically strained along the \hat{z} direction as follows:

$$\varepsilon(t) = \varepsilon_0 \sin(2\pi t/T), \quad (2)$$

where ε_0 is the strain amplitude and the oscillation period is $T = 5000\tau$. The deformation of the simulation cell involved continuous expansion and contraction of the lateral dimensions (along the \hat{x} and \hat{y} axes), so that the total volume remained constant, the so-called pure shear deformation. The simulations were performed at strain amplitudes, $\varepsilon_0 \leq 0.04$, in the elastic range at $\rho = 1.2\sigma^{-3}$ and $T_{LJ} = 0.01\varepsilon/k_B$. For each value of the strain amplitude, the glass was subjected to 1400 back-and-forth cycles. During production runs, the potential energy, stress components, and atomic positions were periodically saved for further analysis. The data were collected only for one realization of disorder due to computational constraints.

III. RESULTS

It is well known that dynamic response of disordered solids to applied mechanical stress or strain depends crucially on the sample processing history [5]. In general, after extended

time intervals at temperatures not far below the glass transition temperature, the amorphous samples become denser and relocate to lower energy states, whereas rapid cooling from the liquid phase to low temperatures usually leads to higher energy, less dense states [5]. The characteristic feature of mechanical deformation of relaxed glasses is the appearance of the stress overshoot at the yielding transition [32]. It was originally shown that during one subyield shear cycle, the potential energy landscape becomes tilted, which allows for a collective rearrangement of groups of atoms to nearby minima, thus leading to a lower energy state upon strain reversal [33]. In the present study, we explore the relaxation process in binary alloys during repeated tension-compression deformation and examine the resulting changes in mechanical properties.

The time dependence of the potential energy minima (at the end of each cycle) is presented in Fig. 1 for the strain amplitudes, $0 \leq \varepsilon_0 \leq 0.04$, in the elastic range. The data for the undeformed glass (at $\varepsilon_0 = 0$) represent the aging process at constant volume, and it shows that the potential energy remains essentially constant during the time interval of $1400 T$. By contrast, it can be clearly observed that periodic deformation at larger strain amplitudes results in deeper energy minima. The lowest value of the potential energy, $U \approx -8.284 \varepsilon$, is attained at $\varepsilon_0 = 0.04$ at $t \approx 1400 T$. Interestingly, this value is nearly the same as the potential energy level reported in the previous study on periodic shear strain along a single plane at the strain amplitude, $\gamma_0 = 0.065$, just below the yielding strain [27]. We also find that the strain amplitude $\varepsilon_0 = 0.05$ is greater than the critical strain amplitude, and the periodic deformation of the glassy material involves extended plastic flow and shear band formation after about 20 cycles (not shown).

It should be noted that the potential energy minima are plotted in Fig. 1 starting from the first cycle, *i.e.*, $t = T$. The potential energy right after rapid cooling but before cyclic loading is $U \approx -8.20 \varepsilon$ (not shown), and after the first cycle it is reduced to $U \approx -8.24 \varepsilon$, depending on the strain amplitude (see Fig. 1). In other words, upon rapid cooling, the glass is settled at a relatively high energy state, and during the first period (either at mechanical equilibrium, $\varepsilon_0 = 0$, or periodically strained, $\varepsilon_0 > 0$) the samples relax to $U \approx -8.24 \varepsilon$ via large-scale particle rearrangements, and only then a more gradual relaxation process begins (as shown in Fig. 1). Therefore, in the following analysis of the relaxation dynamics, the reference configuration of atoms is taken at $t = T$ for each value of the strain amplitude.

The microscopic details of the structural relaxation dynamics during cyclic loading can be inspected via the analysis of the so-called nonaffine displacements of atoms. Recall that atomic displacements in deformed crystalline solids is defined with respect to the periodic lattice. By contrast, the local displacement of atoms in disordered materials can be measured with respect to their neighbors. In this case, the displacement consists of two parts, *i.e.*, affine and nonaffine components. In turn, the nonaffine part can be computed numerically using the transformation matrix \mathbf{J}_i , which linearly transforms a group of neighbors around the atom i during the time interval Δt and, at the same time, minimizes the quantity:

$$D^2(t, \Delta t) = \frac{1}{N_i} \sum_{j=1}^{N_i} \left\{ \mathbf{r}_j(t + \Delta t) - \mathbf{r}_i(t + \Delta t) - \mathbf{J}_i [\mathbf{r}_j(t) - \mathbf{r}_i(t)] \right\}^2, \quad (3)$$

where the summation is carried over the neighboring atoms within a sphere of radius 1.5σ located at $\mathbf{r}_i(t)$. In the original study, Falk and Langer showed that the nonaffine measure, given by Eq. (3), is an excellent diagnostic for detecting local shear transformations when the time interval Δt is properly chosen [34]. In the last several years, the analysis on nonaffine displacements was applied to amorphous materials subjected to time periodic deformation [12, 14, 16, 19, 21, 22, 27], elastostatic loading [39], and thermal cycling [35–38]. In particular, it was found that during periodic shear deformation at strain amplitudes above the critical value, both well and poorly annealed glasses undergo a yielding transition after a number of transient cycles [16, 21]. Moreover, the spatial distribution of nonaffine displacements changes from a set of disconnected clusters of mobile atoms to a localized shear band [16, 21, 28].

The data for the potential energy reported in Fig. 1 indicate that the relaxation dynamics for each value of the strain amplitude slows down as the cycle number increases. This, in turn, implies that the typical size of regions, where atoms undergo irreversible displacements to lower energy states, should also be reduced over time. The sequence of snapshots of atoms with relatively large nonaffine displacements, $D^2(nT, T) > 0.04\sigma^2$, are shown in Fig. 2 for the strain amplitude $\varepsilon_0 = 0.03$ and in Fig. 3 for $\varepsilon_0 = 0.04$. Here, the nonaffine displacements, Eq. (3), were computed for pairs of configurations at zero strain separated by the time interval $\Delta t = T$, where $T = 5000\tau$ is the oscillation period. It can be clearly observed in Figs. 2 and 3 that the initial stage of relaxation involves percolating clusters of mobile atoms, and their typical size is gradually reduced as the cycle number increases. Note that after 1000 cycles at $\varepsilon_0 = 0.03$, shown in Fig. 2 (d), almost all atoms remained inside cages

formed by their neighbors during one cycle. For reference, the cage size at $\rho = 1.2 \sigma^{-3}$ is about 0.1σ [12, 14, 29]. This behavior is consistent with the results of previous MD studies on periodic shear deformation of poorly annealed binary glasses, where it was shown that the volume occupied by atoms with large nonaffine displacements is decreased over time if the strain amplitude is below the critical value [19, 21].

The probability distribution functions of nonaffine displacements are plotted in Figs. 4 and 5 for the strain amplitude $\varepsilon_0 = 0.03$ and in Figs. 6 and 7 for $\varepsilon_0 = 0.04$. In both cases, the nonaffine displacements were computed with respect to the configurations at $t_1 = T$ during time intervals when the decay of the potential energy in Fig. 1 is roughly linear (on the log-normal scale). More specifically, the time interval is $\Delta t \lesssim 200 T$ for $\varepsilon_0 = 0.03$ and $\Delta t \lesssim 600 T$ for $\varepsilon_0 = 0.04$. It can be seen in Figs. 4(a) and 6(a) that the distributions become relatively broad already at $\Delta t = T$, which correlates well with the appearance of large clusters in Figs. 2(a) and 3(a). As expected, the width of the distributions increases at larger time intervals (see Figs. 4 and 6), which reflects larger displacements of atoms with respect to their neighbors at time $t_1 = T$. Interestingly, the probability distribution of the nonaffine measure divided by its averaged value gradually evolves towards a function that does not depend on the cycle number, as shown in Figs. 5 and 7. The common shape of the distribution functions of $D^2/\langle D^2 \rangle$ is most probably related to a weak correlation between atomic configurations separated by a large time interval Δt . In other words, most of the atoms undergo multiple cage jumps, and the neighbors of an atom at $t_1 = T$ are displaced independently over sufficiently large Δt . Note, however, that the slopes of the power-law decay are slightly different for $\varepsilon_0 = 0.03$ and 0.04 .

We next discuss the effect of cyclic loading at different strain amplitudes on the mechanical properties of binary glasses. As shown in Fig. 1, upon increasing strain amplitude within the elastic range, the systems are gradually relocated to lower energy states. After 1400 cycles, the glass was subjected to startup shear deformation along the yz plane with the computationally slow rate $\dot{\gamma}_{yz} = 10^{-5} \tau^{-1}$. The shear stress-strain curves are reported in Fig. 8 for glasses that were annealed during $1400 T$ and loaded during 1400 cycles at $T_{LJ} = 0.01 \varepsilon/k_B$. It can be observed that with increasing strain amplitude of the cyclic loading, ε_0 , the initial slope of the shear stress increases and a pronounced yielding peak is developed at the shear strain $\gamma_{yz} \approx 0.09$. These trends are consistent with the dependence

of the mechanical response of disordered solids on the degree of relaxation; namely, more relaxed glasses are stronger and more brittle [5].

The dependence of the yielding peak, σ_Y , and shear modulus, G , as functions of the strain amplitude is summarized in the insets of Fig. 8. Here, the shear modulus was computed from the slope of the linear fit of the stress-strain curves at $\gamma_{yz} \leq 0.01$, and the data were averaged over three mutually perpendicular planes of shear. In the insets, the dashed lines indicate the averaged values of σ_Y and G before the cyclic loading was applied, whereas the data for $\varepsilon_0 = 0$ were taken in quiescent samples annealed during the time interval $1400 T$. It can be clearly seen that both the stress overshoot and the shear modulus increase at larger strain amplitudes, which is in agreement with the trend reported for the potential energy in Fig. 1. Furthermore, the spatial distributions of nonaffine displacements during startup shear deformation are shown for the annealed sample in Fig. 9 and for the periodically deformed glass in Fig. 10. As is evident, the processing history results in a distinct difference in the deformation pattern, *i.e.*, a nearly homogeneous deformation of rapidly quenched and then thermally annealed sample, and the appearance of the shear band in the cyclicly annealed glass.

IV. CONCLUSIONS

In summary, we carried out molecular dynamics simulations to study the relaxation dynamics in disordered solids subjected to tension-compression cyclic loading and its effect on mechanical properties. The model glass was represented via a binary mixture with strongly non-additive cross interactions that prevent crystallization upon cooling. The binary mixture was rapidly quenched from the liquid phase to the glass phase at a temperature well below the glass transition temperature. The deformation protocol included periodic tension-compression deformation at constant volume during hundreds of cycles. During cyclic loading, the amorphous systems were driven to progressively lower potential energy states via collective nonaffine rearrangements of atoms. Moreover, it was shown that the shape of the rescaled probability distribution function becomes time independent after sufficiently large number of cycles. After cyclic loading, the mechanical properties were probed during startup shear deformation at a constant strain rate. The results of numerical simulations indicate that both the shear modulus and the peak value of the stress overshoot increase in

glasses that were periodically loaded with larger strain amplitudes within the elastic range.

Acknowledgments

Funding from the National Science Foundation (CNS-1531923) is gratefully acknowledged. The molecular dynamics simulations were performed using the LAMMPS open-source code developed at Sandia National Laboratories [30]. The simulations were performed at Wright State University's Computing Facility and the Ohio Supercomputer Center.

-
- [1] M. M. Khan, A. Nemati, Z. U. Rahman, U. H. Shah, H. Asgar, and W. Haider, Recent Advancements in Bulk Metallic Glasses and Their Applications: A Review, *Crit. Rev. Solid State Mater. Sci.* **43**, 233 (2018).
 - [2] F. Spaepen, A microscopic mechanism for steady state inhomogeneous flow in metallic glasses, *Acta Metall.* **25**, 407 (1977).
 - [3] A. S. Argon, Plastic deformation in metallic glasses, *Acta Metall.* **27**, 47 (1979).
 - [4] T. Egami, T. Iwashita, and W. Dmowski, Mechanical properties of metallic glasses, *Metals* **3**, 77 (2013).
 - [5] Y. Sun, A. Concustell, and A. L. Greer, Thermomechanical processing of metallic glasses: Extending the range of the glassy state, *Nat. Rev. Mater.* **1**, 16039 (2016).
 - [6] N. V. Priezjev, Heterogeneous relaxation dynamics in amorphous materials under cyclic loading, *Phys. Rev. E* **87**, 052302 (2013).
 - [7] D. Fiocco, G. Foffi, and S. Sastry, Oscillatory athermal quasistatic deformation of a model glass, *Phys. Rev. E* **88**, 020301(R) (2013).
 - [8] I. Regev, T. Lookman, and C. Reichhardt, Onset of irreversibility and chaos in amorphous solids under periodic shear, *Phys. Rev. E* **88**, 062401 (2013).
 - [9] N. V. Priezjev, Dynamical heterogeneity in periodically deformed polymer glasses, *Phys. Rev. E* **89**, 012601 (2014).
 - [10] J. Luo, K. Dahmen, P. K. Liaw, and Y. Shi, Low-cycle fatigue of metallic glass nanowires, *Acta Mater.* **87**, 225 (2015).
 - [11] Y. F. Ye, S. Wang, J. Fan, C. T. Liu, and Y. Yang, Atomistic mechanism of elastic softening in

- metallic glass under cyclic loading revealed by molecular dynamics simulations, *Intermetallics* **68**, 5 (2016).
- [12] N. V. Priezjev, Reversible plastic events during oscillatory deformation of amorphous solids, *Phys. Rev. E* **93**, 013001 (2016).
 - [13] T. Kawasaki and L. Berthier, Macroscopic yielding in jammed solids is accompanied by a non-equilibrium first-order transition in particle trajectories, *Phys. Rev. E* **94**, 022615 (2016).
 - [14] N. V. Priezjev, Nonaffine rearrangements of atoms in deformed and quiescent binary glasses, *Phys. Rev. E* **94**, 023004 (2016).
 - [15] P. Leishangthem, A. D. S. Parmar, and S. Sastry, The yielding transition in amorphous solids under oscillatory shear deformation, *Nat. Commun.* **8**, 14653 (2017).
 - [16] N. V. Priezjev, Collective nonaffine displacements in amorphous materials during large-amplitude oscillatory shear, *Phys. Rev. E* **95**, 023002 (2017).
 - [17] P. K. Jana, M. J. Alava, and S. Zapperi, Irreversibility transition of colloidal polycrystals under cyclic deformation, *Sci. Rep.* **7**, 45550 (2017).
 - [18] S. Dagois-Bohy, E. Somfai, B. P. Tighe, and M. van Hecke, Softening and yielding of soft glassy materials, *Soft Matter* **13**, 9036 (2017).
 - [19] N. V. Priezjev, Molecular dynamics simulations of the mechanical annealing process in metallic glasses: Effects of strain amplitude and temperature, *J. Non-Cryst. Solids* **479**, 42 (2018).
 - [20] P. K. Jana, M. J. Alava, and S. Zapperi, Irreversible transition of amorphous and polycrystalline colloidal solids under cyclic deformation, *Phys. Rev. E* **98**, 062607 (2018).
 - [21] N. V. Priezjev, The yielding transition in periodically sheared binary glasses at finite temperature, *Comput. Mater. Sci.* **150**, 162 (2018).
 - [22] N. V. Priezjev, Slow relaxation dynamics in binary glasses during stress-controlled, tension-compression cyclic loading, *Comput. Mater. Sci.* **153**, 235 (2018).
 - [23] Y. Bai and C. She, Atomic structure evolution in metallic glasses under cyclic deformation, *Comput. Mater. Sci.* **169**, 109094 (2019).
 - [24] N. V. Priezjev and M. A. Makeev, The influence of periodic shear on structural relaxation and pore redistribution in binary glasses, *J. Non-Cryst. Solids* **506**, 14 (2019).
 - [25] N. V. Priezjev and M. A. Makeev, Structural transformations during periodic deformation of low-porosity amorphous materials, *Modelling Simul. Mater. Sci. Eng.* **27**, 025004 (2019).
 - [26] M. Zhang, Q. Li, J. Zhang, X. Wang, J. Jin, P. Gong, and L. Deng, Influence of vibrational

- loading on deformation behavior of metallic glass: A molecular dynamics study, *Metals* **9**, 1197 (2019).
- [27] N. V. Priezjev, Accelerated relaxation in disordered solids under cyclic loading with alternating shear orientation, *J. Non-Cryst. Solids* **525**, 119683 (2019).
 - [28] N. V. Priezjev, Shear band formation in amorphous materials under oscillatory shear deformation, arXiv:1911.06157
 - [29] W. Kob and H. C. Andersen, Testing mode-coupling theory for a supercooled binary Lennard-Jones mixture: The van Hove correlation function, *Phys. Rev. E* **51**, 4626 (1995).
 - [30] S. J. Plimpton, Fast parallel algorithms for short-range molecular dynamics, *J. Comp. Phys.* **117**, 1 (1995).
 - [31] M. P. Allen and D. J. Tildesley, *Computer Simulation of Liquids* (Clarendon, Oxford, 1987).
 - [32] M. Utz, P. G. Debenedetti, and F. H. Stillinger, Atomistic simulation of aging and rejuvenation in glasses, *Phys. Rev. Lett.* **84**, 1471 (2000).
 - [33] D. J. Lacks and M. J. Osborne, Energy landscape picture of overaging and rejuvenation in a sheared glass, *Phys. Rev. Lett.* **93**, 255501 (2004).
 - [34] M. L. Falk and J. S. Langer, Dynamics of viscoplastic deformation in amorphous solids, *Phys. Rev. E* **57**, 7192 (1998).
 - [35] N. V. Priezjev, The effect of cryogenic thermal cycling on aging, rejuvenation, and mechanical properties of metallic glasses, *J. Non-Cryst. Solids* **503**, 131 (2019).
 - [36] Q.-L. Liu and N. V. Priezjev, The influence of complex thermal treatment on mechanical properties of amorphous materials, *Comput. Mater. Sci.* **161**, 93 (2019).
 - [37] N. V. Priezjev, Potential energy states and mechanical properties of thermally cycled binary glasses, *J. Mater. Res.* **34**, 2664 (2019).
 - [38] N. V. Priezjev, Atomistic modeling of heat treatment processes for tuning the mechanical properties of disordered solids, *J. Non-Cryst. Solids* **518**, 128 (2019).
 - [39] N. V. Priezjev, Aging and rejuvenation during elastostatic loading of amorphous alloys: A molecular dynamics simulation study, *Comput. Mater. Sci.* **168**, 125 (2019).

Figures

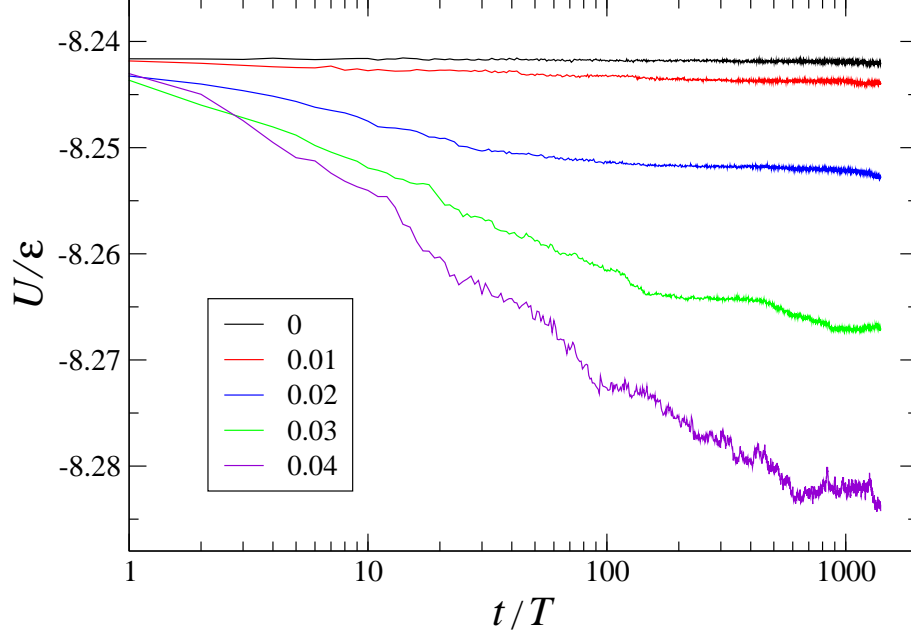


FIG. 1: (Color online) The potential energy minima at the end of each cycle for the strain amplitudes $\varepsilon_0 = 0$ (black), 0.01 (red), 0.02 (blue), 0.03 (green), and 0.04 (violet), from top to bottom. The period of cyclic deformation is $T = 5000\tau$ and the system temperature is $T_{LJ} = 0.01\varepsilon/k_B$. The data for $\varepsilon_0 = 0$ correspond to the quiescent glass annealed during the time interval $1400T$.

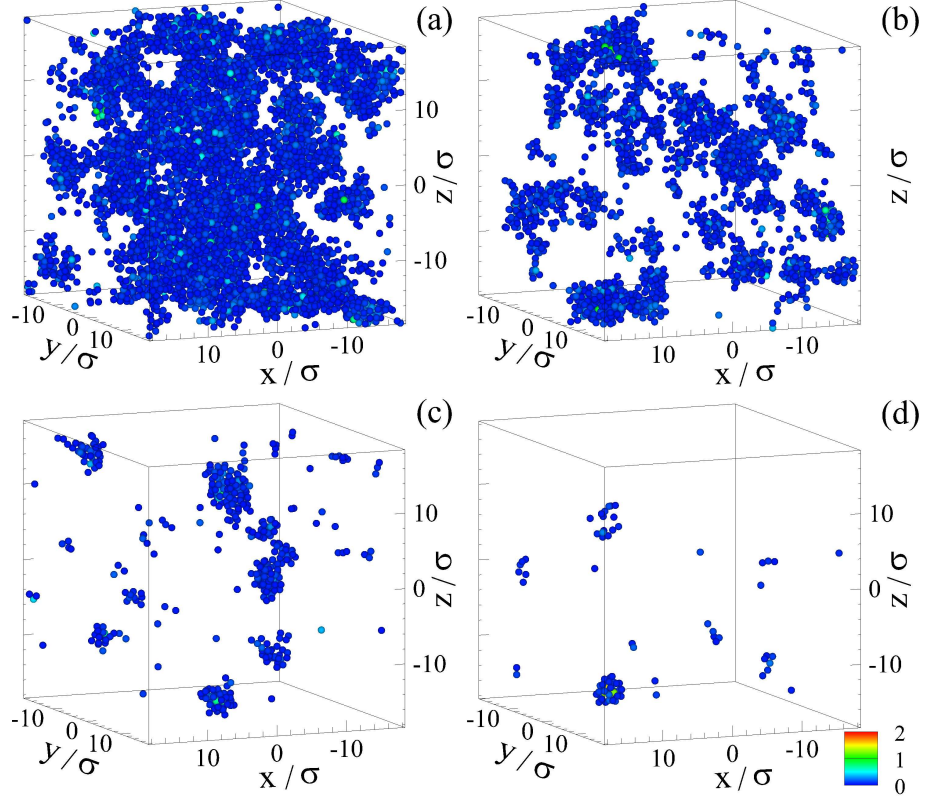


FIG. 2: (Color online) The positions of atoms with large nonaffine measure (a) $D^2(T, T) > 0.04\sigma^2$, (b) $D^2(10T, T) > 0.04\sigma^2$, (c) $D^2(100T, T) > 0.04\sigma^2$, and (d) $D^2(1000T, T) > 0.04\sigma^2$. The color code for $D^2(nT, T)$ is defined in the legend. The strain amplitude is $\varepsilon_0 = 0.03$ and the oscillation period is $T = 5000\tau$.

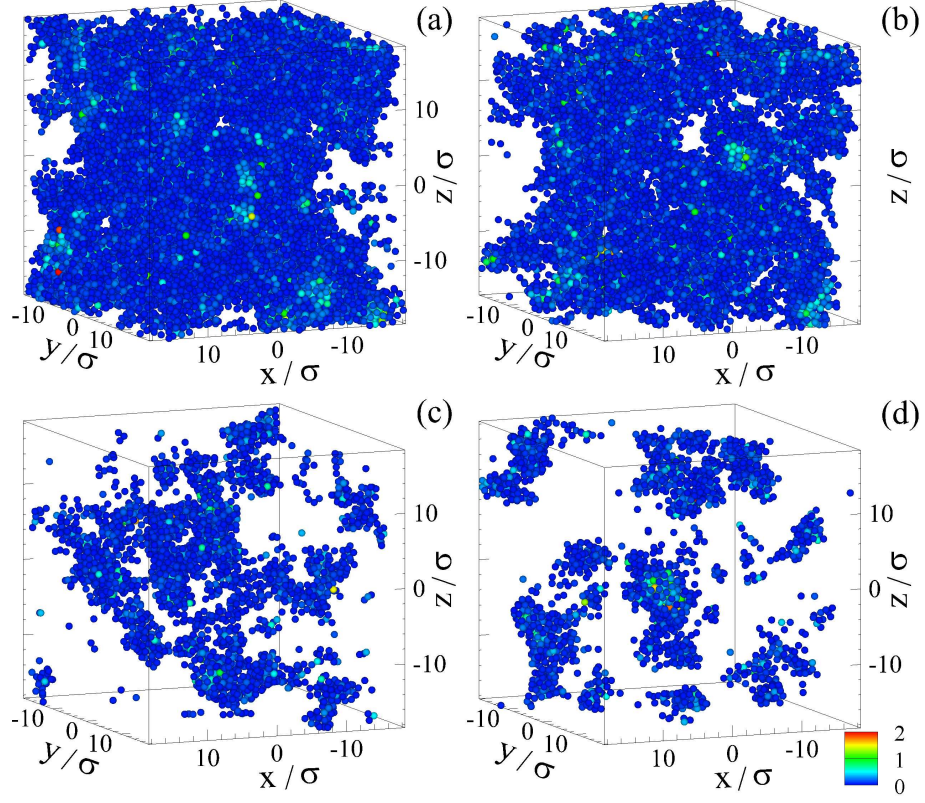


FIG. 3: (Color online) The sequence of snapshots of atoms with the nonaffine measure (a) $D^2(T, T) > 0.04\sigma^2$, (b) $D^2(10T, T) > 0.04\sigma^2$, (c) $D^2(100T, T) > 0.04\sigma^2$, and (d) $D^2(1000T, T) > 0.04\sigma^2$. The atoms are colored according to the legend. The oscillation period is $T = 5000\tau$ and the strain amplitude is $\varepsilon_0 = 0.04$.

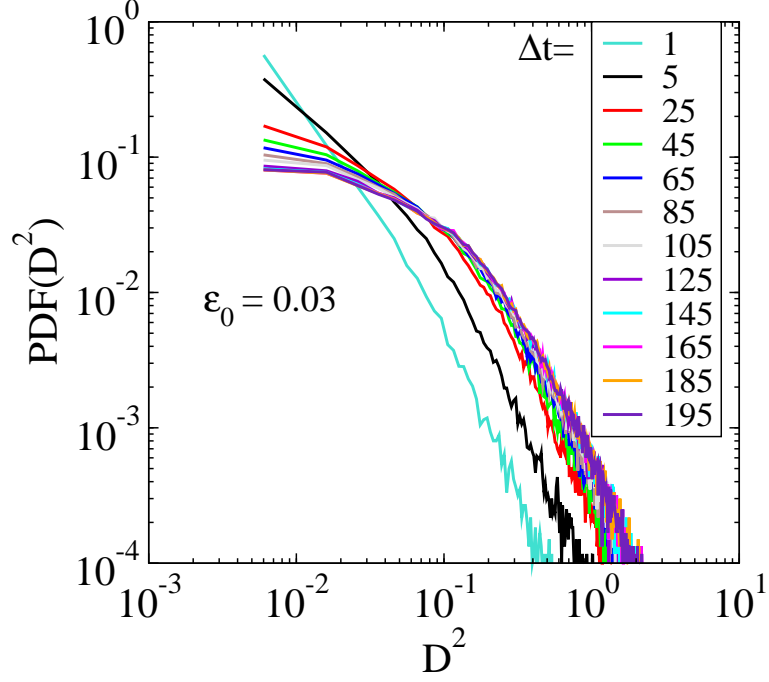


FIG. 4: (Color online) The distribution of nonaffine quantity $D^2(t_1, \Delta t)$ for the strain amplitude $\varepsilon_0 = 0.03$. The legend shows time intervals Δt , measured in oscillation periods ($T = 5000 \tau$), with respect to the atomic configuration at $t_1 = T$.

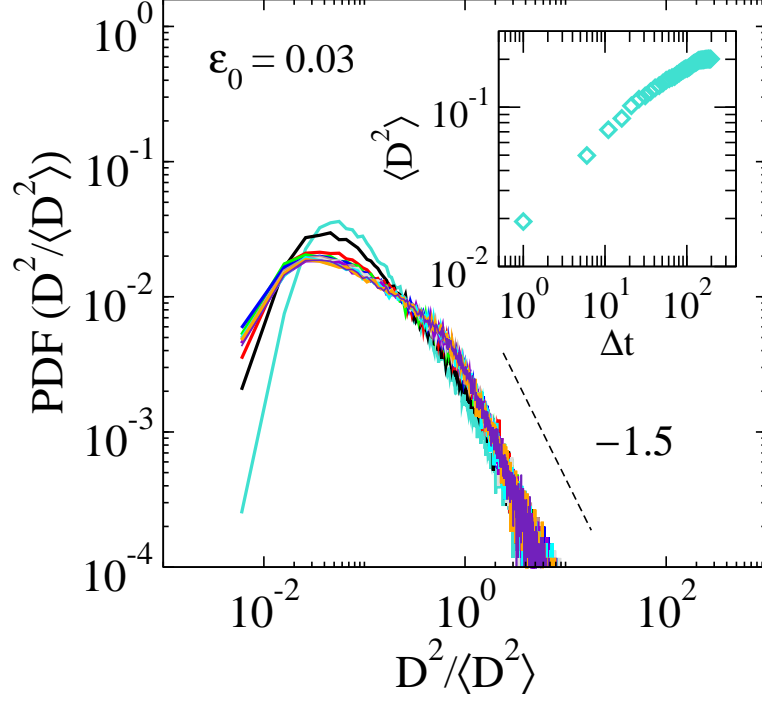


FIG. 5: (Color online) The rescaled distribution of $D^2(t_1, \Delta t)$ for the strain amplitude $\varepsilon_0 = 0.03$. The same data and color code as in Fig. 4. The dashed line indicates the slope -1.5 . The inset shows the average of $D^2(t_1, \Delta t)$ as a function of the time interval Δt .

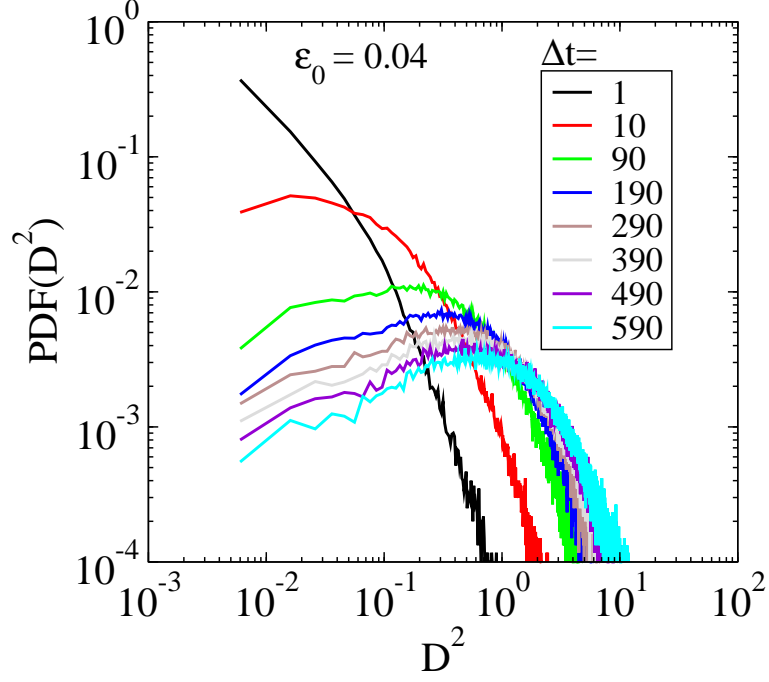


FIG. 6: (Color online) The probability distribution of the nonaffine measure $D^2(t_1, \Delta t)$ for the strain amplitude $\varepsilon_0 = 0.04$. The values of the time interval Δt are listed in the table. The reference state is $t_1 = T$, where $T = 5000 \tau$ is the period of cyclic loading.

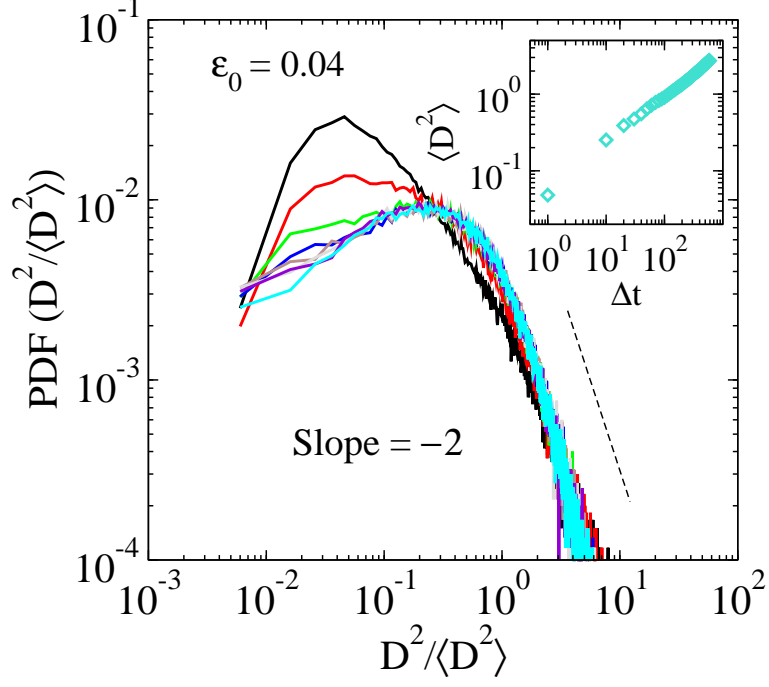


FIG. 7: (Color online) The distribution of $D^2(t_1, \Delta t)$ divided by its average for the strain amplitude $\varepsilon_0 = 0.04$. The color code is the same as in Fig. 6. The slope -2 is shown for reference. The average value of $D^2(t_1, \Delta t)$ versus Δt is reported in the inset.

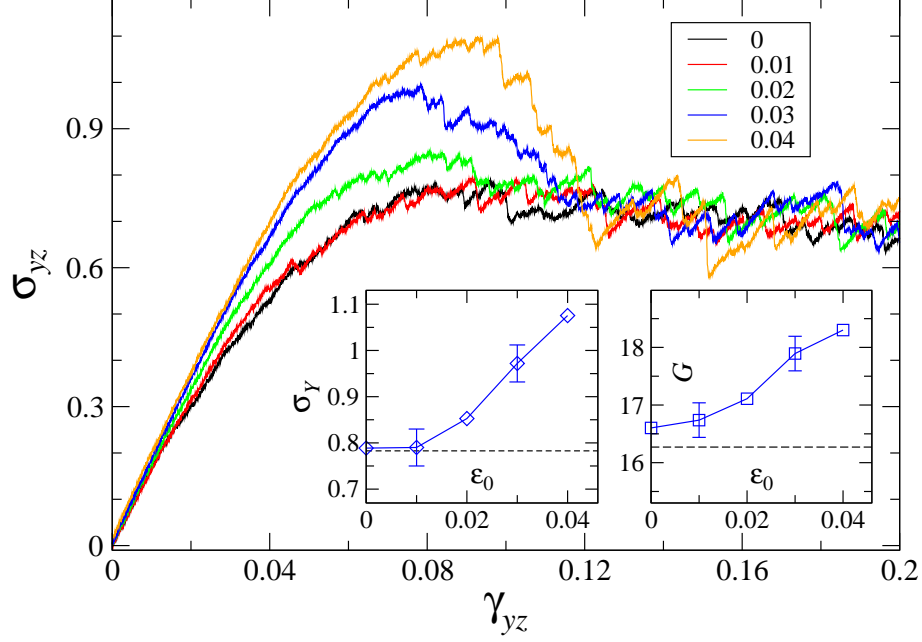


FIG. 8: (Color online) The variation of shear stress, σ_{yz} (in units of $\varepsilon\sigma^{-3}$) during steady strain with the rate $10^{-5}\tau^{-1}$. The glasses were strained after 1400 tension-compression cycles with the indicated strain amplitudes. The insets show the yielding peak, σ_Y (in units of $\varepsilon\sigma^{-3}$), and the shear modulus, G (in units of $\varepsilon\sigma^{-3}$), as functions of the strain amplitude. The horizontal dashed lines in the insets indicate σ_Y and G before periodic loading was applied.

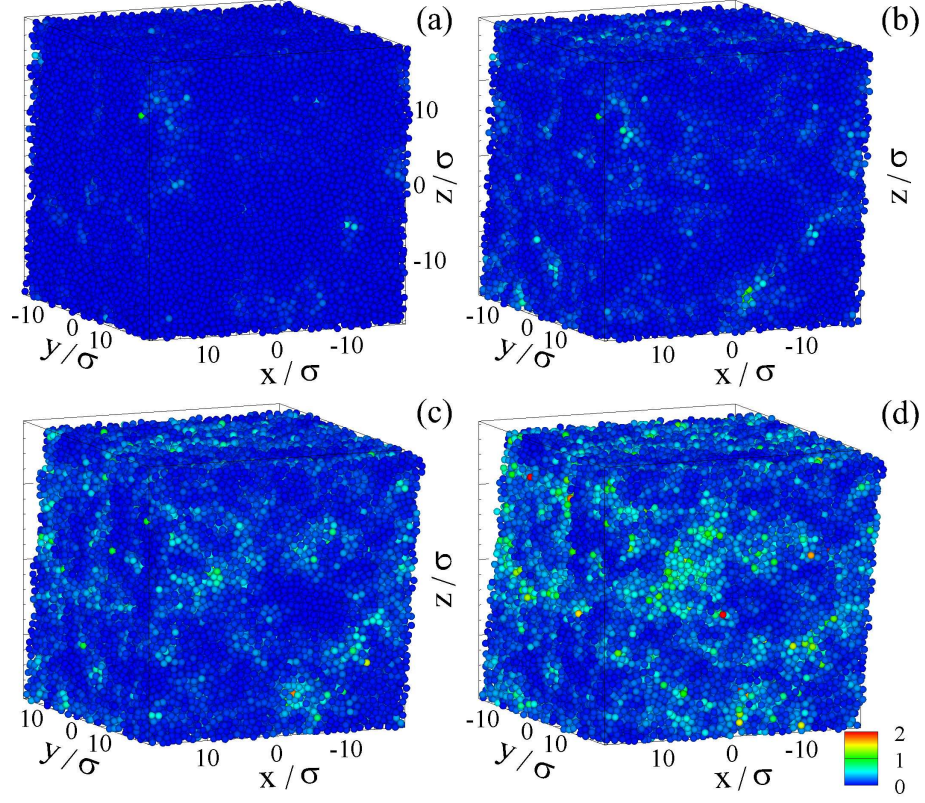


FIG. 9: (Color online) The snapshots of the binary glass that was annealed during $1400T$ at $T_{LJ} = 0.01 \varepsilon/k_B$ and then sheared along the yz plane with the rate of $10^{-5} \tau^{-1}$. The shear strain is (a) 0.05, (b) 0.10, (c) 0.15, and (d) 0.20. The color denotes D^2 with respect to the atomic configuration at zero strain.

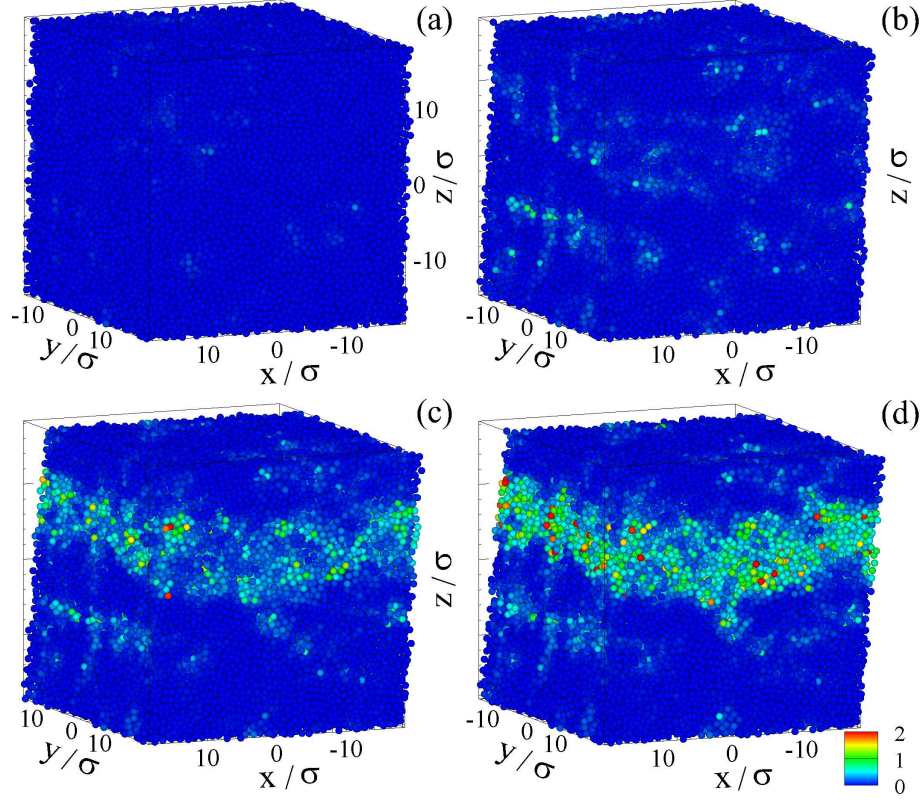


FIG. 10: (Color online) The atomic configurations of the strained glass after 1400 tension-compression cycles with the strain amplitude $\varepsilon_0 = 0.04$. The shear strain, γ_{yz} , is (a) 0.05, (b) 0.10, (c) 0.15, and (d) 0.20. The color of atoms indicates their nonaffine displacements with respect to $\gamma_{yz} = 0$, see the legend.